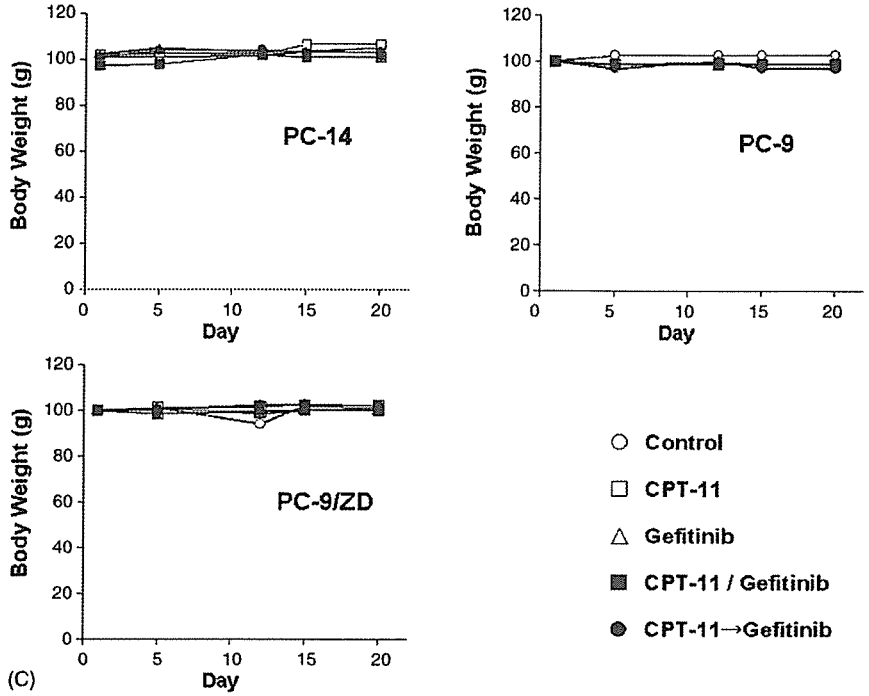

Fig. 2 (*Continued*).

ment of lung cancers expressing wild-type EGFR is a major obstacle. Combined therapies are still considered to be a major strategy against lung cancer expressing wild-type EGFR. Our previous preclinical study demonstrated that gefitinib and CPT-11 have synergistic effects in colorectal cancer cell lines [14]. Here, we reevaluated the combined effects of gefitinib and cytotoxic agents based on the status of EGFR mutations in lung cancer.

We demonstrated that gefitinib and SN-38, the active form of CPT-11, have synergistic or additive effects in lung cancer cells expressing wild-type EGFR. The combination of gefitinib and CPT-11 may be useful against lung cancers expressing wild-type EGFR. On the other hand, this combination had antagonistic effects in PC-9 cells expressing mutant EGFR, even though PC-9 cells are basically hypersensitive to gefitinib alone.

The concurrent administration of gefitinib and SN-38 also had an antagonistic effect in the PC-9/ZD cells. The PC-9/ZD cells developed an acquired resistance to gefitinib after exposure to gefitinib in vitro. New treatment strategies for patients who are refractory to gefitinib treatment are clinically needed. We demonstrated that the sequential administration of SN-38 (CPT-11) and gefitinib improved the combined effects in PC-9/ZD cells both in vitro and in vivo.

The above results led us to propose a combined gefitinib and CPT-11 treatment strategy based on the EGFR mutation status of lung cancers: (1) combined treatment according to any schedule for lung cancers expressing wild-type EGFR, (2) gefitinib treatment alone for lung cancers expressing mutant EGFR, and (3) the sequential administration of gefitinib and CPT-11 for patients who are refractory to gefitinib treatment. Based on the above preclinical evidence, we are preparing to begin a clinical phase II trial for combined gefitinib and CPT-11 treatment in Japan.

We previously demonstrated that CPT-11 and gefitinib have a synergistic effect against colorectal cancer [14]. EGFR mutations are rarely observed in colorectal cancer cells [15]. Therefore, the combined effects of these agents against colorectal cancers were consistent with those against the lung cancers expressing wild-type EGFR in this study.

Different combined effects were observed for the concurrent and sequential schedules in vitro and in vivo. While the mechanisms responsible for the combined effects remain unclear, cell cycle distributions might explain some of the differences. In cells treated according to the sequential gefitinib followed by SN-38 (CPT-11) treatment schedule, treatment with gefitinib resulted in an increase in the G0–G1 phase and a decrease in the S phase populations (data not shown). The decreased S phase population was not sensitive to CPT-11 [16]. Thus, the antagonistic effects of the sequential administration of gefitinib followed by CPT-11 (SN-38) could be explained by this mechanism. On the other hand, in cells treated according to the sequential SN-38 followed by gefitinib treatment schedule, SN-38 treatment induced an increase in the S phase population. If the S phase population is sensitive to gefitinib, this might explain the synergistic effects of this sequential schedule [17]. An increase in EGFR phosphorylation induced by CPT-11 is another previously reported possible mechanism responsible for this synergistic action [14].

In conclusion, we demonstrated the different effect on lung cancer cell expressing mutant EGFR according to the

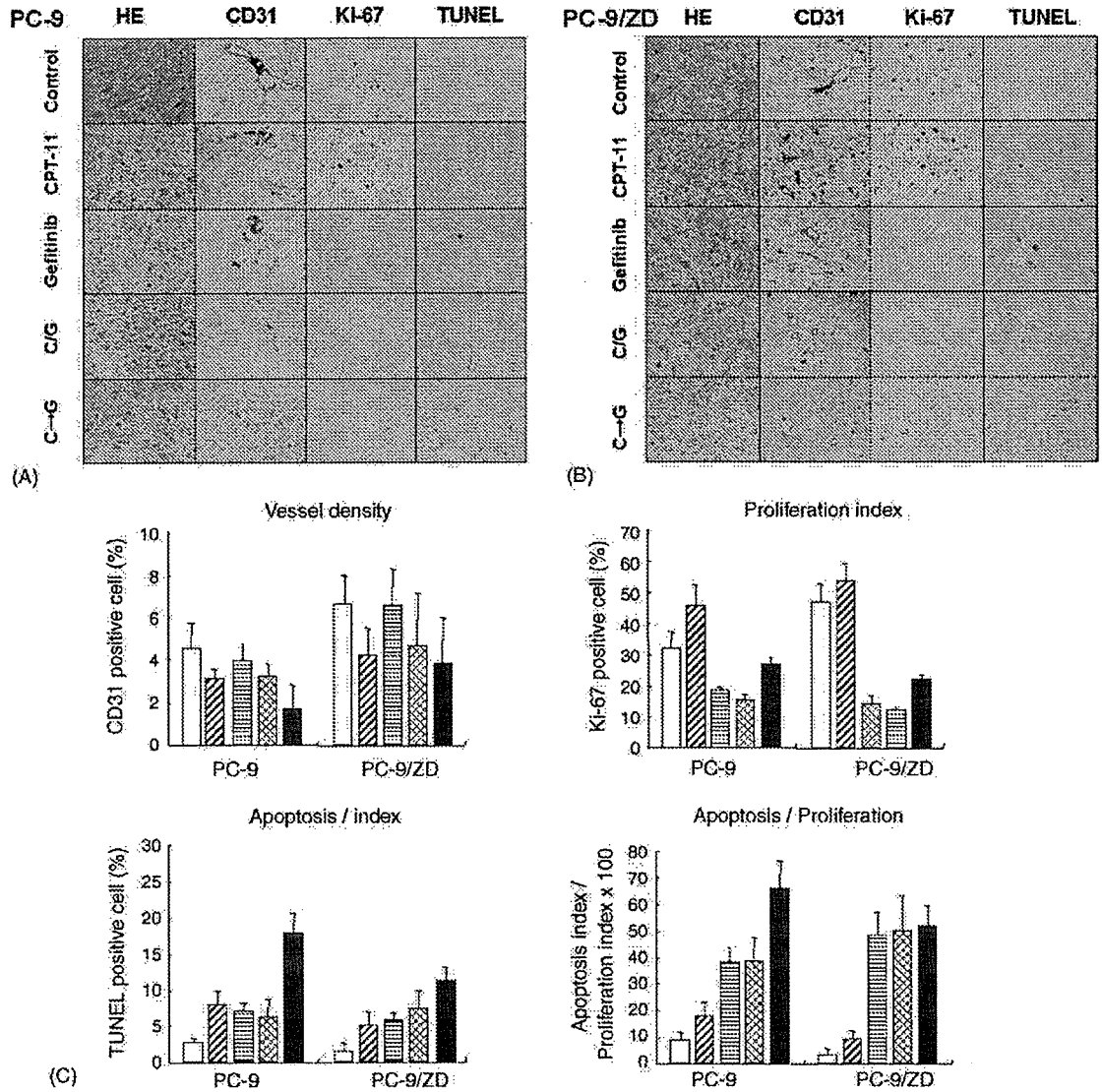

Fig. 3 (A) Historical examination of PC-9 tumor xenografts (day 22) stained with H&E, anti-CD31 vessel staining, TUNEL staining (magnification: 400×) and anti-Ki-67 nuclear antigen (magnification: 200×). The number of Ki-67-positive cells increased with the administration of CPT-11. The number of Ki-67-positive cells decreased with the gefitinib-alone and combination treatments. C/G: concurrent combination, C → G: sequential combination. (B) Historical examination of PC-9ZD tumor xenografts (day 22) stained with H&E, anti-CD31 vessel staining, TUNEL staining (magnification: 400×) and anti-Ki-67 nuclear antigen (magnification: 200×). The number of Ki-67-positive cells increased with the administration of CPT-11. The number of Ki-67-positive cells decreased with the gefitinib-alone and combination treatments. C → G: sequential combination; C/G: concurrent combination. (C) Quantitation of CD31 vessel staining, Ki-67 proliferation index, apoptosis index, and apoptosis: proliferation ratio. The columns represent the mean population of positive cells in five fields. Bars: ±S.D. Tumors from mice treated with vehicle (white), CPT-11 (diagonal hatched), Gefitinib (horizontal hatched), concurrent combination of CPT-11 plus Gefitinib (cross-hatched), or sequential combination of CPT-11 plus Gefitinib (cross-hatched).

combination schedule of gefitinib and CPT-11. The sequential combined treatment also active against lung cancer cell expressing wild-type EGFR.

Acknowledgements

This study was supported in part by a Grant-in-Aid for Cancer Research and the 3rd Term Comprehensive 10-Year Strategy for Cancer Control from the Ministry of Health, Labour and Welfare, Tokyo, Japan.

References

[1] Lynch TJ, Bell DW, Sordella R, Gurubhagavatula S, Okimoto RA, Brannigan BW, et al. Activating mutations in the epidermal growth factor receptor underlying responsiveness of non-small-

cell lung cancer to gefitinib. N Engl J Med 2004;350:2129–39.
[2] Paez JG, Janne PA, Lee JC, Tracy S, Greulich H, Gabriel S, et al. EGFR mutations in lung cancer: correlation with clinical response to gefitinib therapy. Science 2004;304:1497–500.
[3] Kobayashi S, Boggon TJ, Dayaram T, Janne PA, Kocher O, Meyerson M, et al. EGFR mutation and resistance of non-small-cell lung cancer to gefitinib. N Engl J Med 2005;352:786–92.
[4] Koizumi F, Shimoyama T, Taguchi F, Saijo N, Nishio K, Kanzawa F, et al. Establishment of a human non-small cell lung cancer cell line resistant to gefitinib Synergistic interaction between the EGFR tyrosine kinase inhibitor gefitinib ("Iressa") and the DNA topoisomerase I inhibitor CPT-11 (irinotecan) in human colorectal cancer cells. Int J Cancer 2005;116:36–44.
[5] Naruse I, Ohmori T, Ao Y, Fukumoto H, Kuroki T, Mori M, et al. Antitumor activity of the selective epidermal growth factor receptor-tyrosine kinase inhibitor (EGFR-TKI) Iressa (ZD1839) in an EGFR-expressing multidrug-resistant cell line in vitro and in vivo. Int J Cancer 2002;98:310–5.
[6] Kanzawa F, Akiyama Y, Saijo N, Nishio K. In vitro effects of combinations of cis-amminedichloro (2-methylpyridine) platinum(II) (ZD0473) with other novel anticancer drugs on the growth of SBC-3, a human small cell lung cancer cell line. Lung Cancer 2003;40:325–32.
[7] Chou TC, Talalay P. Quantitative analysis of dose-effect relationships: the combined effects of multiple drugs or enzyme inhibitors. Adv Enzyme Regul 1984;22:27–55.
[8] Ciardiello F, Caputo R, Bianco R, Damiano V, Pomatico G, De Placido S, et al. Antitumor effect and potentiation of cytotoxic drugs activity in human cancer cells by ZD-1839 (Iressa), an epidermal growth factor receptor-selective tyrosine kinase inhibitor. Clin Cancer Res 2000;6:2053–63.
[9] Sirotnak FM, Zakowski MF, Miller VA, Scher HI, Kris MG. Efficacy of cytotoxic agents against human tumor xenografts is markedly enhanced by coadministration of ZD1839 (Iressa), an inhibitor of EGFR tyrosine kinase. Clin Cancer Res 2000; 6:4885–92.
[10] Giaccone G, Herbst RS, Manegold C, Scagliotti G, Rosell R, Miller V, et al. Gefitinib in combination with gemcitabine and cisplatin in advanced non-small-cell lung cancer: a phase III trial—INTACT 1. J Clin Oncol 2004;22:777–84.
[11] Herbst RS, Giaccone G, Schiller JH, Natale RB, Miller V, Manegold C, et al. Gefitinib in combination with paclitaxel and carboplatin in advanced non-small-cell lung cancer: a phase III trial—INTACT 2. J Clin Oncol 2004;22:785–94.
[12] Taguchi F, Koh Y, Koizumi F, Tamura T, Saijo N, Nishio K. Anticancer effects of ZD6474, a VEGF receptor tyrosine kinase inhibitor, in gefitinib ("Iressa")-sensitive and resistant xenograft models. Cancer Sci 2004;95:984–9.
[13] Arao T, Fukumoto H, Takeda M, Tamura T, Saijo N, Nishio K. Small in-frame deletion in the epidermal growth factor receptor as a target for ZD6474. Cancer Res 2004;64:9101–4.
[14] Koizumi F, Kanzawa F, Ueda Y, Koh Y, Tsukiyama S, Taguchi F, et al. Synergistic interaction between the EGFR tyrosine kinase inhibitor gefitinib ("Iressa") and the DNA topoisomerase I inhibitor CPT-11 (irinotecan) in human colorectal cancer cells. Int J Cancer 2004;108:464–72.
[15] Barber TD, Vogelstein B, Kinzler KW, Velculescu VE. Somatic mutations of EGFR in colorectal cancers and glioblastomas. N Engl J Med 2004;351:2883.
[16] van Ark-Otte J, Kedde MA, van der Vijgh WJ, Dingemans AM, Jansen WJ, Pinedo HM, et al. Determinants of CPT-11 and SN-38 activities in human lung cancer cells. Br J Cancer 1998;77:2171–6.
[17] Park JK, Lee SH, Kang JH, Nishio K, Saijo N, Kuh HJ. Synergistic interaction between gefitinib (Iressa ZD1839) and paclitaxel against human gastric carcinoma cells. Anticancer Drugs 2004;15:809–18.

High sensitivity detection of *epidermal growth factor receptor* mutations in the pleural effusion of non-small cell lung cancer patients

Hideharu Kimura,[1,2] Yutaka Fujiwara,[3] Takashi Sone,[2] Hideo Kunitoh,[3] Tomohide Tamura,[3] Kazuo Kasahara[2] and Kazuto Nishio[1,4,5,6]

[1]Shien-Laboratory, National Cancer Center Hospital, 5-1-1 Tsukiji, Chuo-ku, Tokyo 104-0045, [2]Respiratory Medicine, Kanazawa University Hospital, 13-1 Takara-machi, Kanazawa, Ishikawa 920-8641, [3]Medical Oncology, National Cancer Center Hospital, Tsukiji 5-1-1, Chuo-ku, Tokyo 104-0045 and [4]Pharmacology Division and [5]Center for Medical Genomics, National Cancer Center Research Institute, Tsukiji 5-1-1, Chuo-ku, Tokyo 104-0045, Japan

(Received January 19, 2006/Revised February 22, 2006/Accepted February 25, 2006/Online publication April 26, 2006)

Epidermal growth factor receptor (EGFR) **mutations are a strong determinant of tumor response to gefitinib in non-small cell lung cancer (NSCLC). We attempted to elucidate the feasibility of *EGFR* mutation detection in cells of pleural effusion fluid. We obtained 24 samples of pleural effusion fluid from NSCLC patients. The pleural effusion fluid was centrifuged, and the cellular components obtained were used for detection. *EGFR* mutation status was determined by a direct sequencing method (exons 18–21) and by the Scorpion Amplified Refractory Mutation System (ARMS) method. *EGFR* mutations were detected in eight cases. Three mutations were detected by both methods, and the other five mutations were detected by Scorpion ARMS alone. The mutations were detected by both methods in all four partial responders among the seven patients who received gefitinib therapy. Direct sequencing detected the mutations in only two of four cases with partial response. These results suggest that the DNA in pleural effusion fluid can be used to detect EGFR mutations. The Scorpion *ARMS* method appears to be more sensitive for detecting *EGFR* mutations than the direct sequencing method. (*Cancer Sci* 2006; 97: 642–648)**

Lung cancer is a major cause of cancer-related mortality worldwide and is expected to remain a major health problem for the foreseeable future.[1] Targeting the epidermal growth factor receptor (EGFR) is one appealing strategy for the treatment of non-small cell lung cancer (NSCLC), because EGFR has been found to be expressed, sometimes strongly, in NSCLC.[2] Mutations of *EGFR* tyrosine kinase in NSCLC and hyper-responsiveness to gefitinib, a selective EGFR tyrosine kinase inhibitor, have been reported.[3,4] These mutations consist of small in-frame deletions or substitutions clustered around the ATP-binding site in exons 18, 19 and 21 of *EGFR*, and increase the affinity of the enzyme for ATP and gefitinib. Some investigators have subsequently found that *EGFR* mutations are a strong determinant of tumor response to EGFR tyrosine kinase inhibitor.[5–7] Approximately 90% of the NSCLC-associated EGFR mutations in two reports consisted of two major *EGFR* mutations (E746_A750del in exon 19 and L858R in exon 21).[5,8] These investigators used surgical tissue to detect the *EGFR* mutations in their trials. As it is often difficult to obtain a tumor sample from patients with inoperable NSCLC, a method of detecting mutant *EGFR*, especially the two major mutations, in other specimens needs to be established.

Malignant pleural effusion is a common complication of lung cancer and is present in approximately 15% of lung cancer patients[9] and in 10–50% of patients at the time of diagnosis.[10] Approximately one-half of NSCLC patients with pleural effusion are initially positive cytologically, and most of the effusions are ultimately determined to be malignant. As sampling of pleural effusion fluid is usually easy, non-invasive and repeatable, we hypothesized that tumor cells in the pleural effusion fluid of NSCLC patients are a source of useful information on the status of the *EGFR* gene with regard to gefitinib response.

Genomic polymerase chain reaction (PCR) and the direct sequencing method have been used widely to detect *EGFR* mutations. It is well known that fusion between normal cells and tumor cells prevents detection of mutations in tumor cells by the direct sequencing method. Therefore it is necessary to enhance sensitivity for detection of *EGFR* mutations in a mixture of normal and tumor cells. We hypothesized that Scorpion Amplified Refractory Mutation System (ARMS) technology enhances sensitivity for detecting *EGFR* mutations. Scorpion primers are used in a fluorescence-based method for specific detection of PCR products.[11] A 'scorpion' consists of a specific probe sequence held in a hairpin loop configuration by complementary stem sequences on the 5′ and 3′ sides of the probe. A scorpion can be used in combination with ARMS to enable detection of single-base mutations.[11,12] The ARMS method was used for allele discrimination, and additional mismatches were introduced near the 3′ terminus of the primers to enhance specificity. A previous study showed that the ARMS method is superior to the direct sequencing method and the WAVE® (Transgenomic Inc., Cambridge, MA, USA) method for the detection of *EGFR* mutations.[13]

In the present study we attempted to detect major *EGFR* mutations in pleural effusion, and to find out whether the Scorpion ARMS method enhances sensitivity for detection of EGFR mutations in mixtures of DNA from normal cells and tumor cells.

[6]To whom correspondence should be addressed.
E-mail: knishio@gan2.res.ncc.go.jp

doi: 10.1111/j.1349-7006.2006.00216.x

Patients and Methods

Patients

We studied NSCLC patients who had a pleural effusion at the time of diagnosis. The diagnosis of NSCLC was based on histological or cytological findings. This study was approved by the Institutional Review Boards of the National Cancer Center Hospital and Kanazawa University Hospital, and written informed consent was obtained from all participants. The patient record consisted of age, sex, smoking habit, histological type of NSCLC and treatment. The response of the patients treated with gefitinib was evaluated in accordance with the 'Response Evaluation Criteria in Solid Tumors (RECIST)' guidelines.[14] No research results were entered into the patient's record or released to the patient or their physician.

Collection of pleural effusion fluid and cell separation

The pleural effusion fluid was collected from patients in heparinized tubes between 29 March and 25 November 2005. No particular collection method was used. Pleural effusion fluid (1 mL) was centrifuged at 250 *g* for 10 min, and the cell pellet was stored at −80°C until use.

DNA extraction

DNA was extracted from the stored cell pellets using a Qiamp DNA Mini Kit (Qiagen, Hilden, Germany) according to the protocol for tissue samples in the manufacturer's instructions. The DNA obtained was eluted in 50 μL of sterile bidistilled buffer, and the concentration and purity of the extracted DNA were assessed by spectrophotometry. The extracted DNA was stored at −20°C until use.

PCR amplification and direct sequencing

Exons 18, 19, 20 and 21 of the *EGFR* gene were amplified by PCR. The primers were designed based on a report by Lynch *et al.*[3] Genomic PCR of 20 ng of template DNA was carried out in 25-μL volumes containing 0.75 IU of Ampli *Taq* Gold DNA polymerase (Roche Molecular Systems, Branchburg, NJ, USA), 2.5 μL of PCR buffer, 0.8 μM dNTP, 0.5 μM of each primer, and different concentrations of $MgCl_2$, depending on the polymorphic marker. The first PCR analyses were carried out in a volume of 25 μL for 25 cycles, consisting of a denaturation step at 94°C for 45 s, a primer annealing step at 58°C for 30 s, and an elongation step at 72°C for 30 s. The final step at 72°C was extended for 10 min. Nested PCR was carried out for 20 cycles under the same conditions as the first PCR. Sequencing of each sample was carried out in duplicate using an ABI prism 310 (Applied Biosystems, Foster City, CA, USA). The sequences were compared with the GenBank-archived human sequence for EGFR (accession number AY588246).

Scorpion ARMS for the detection of E746_A750del and L858R

We used an EGFR Scorpion™ Kit (DxS, Manchester, UK), which combines the two technologies ARMS and Scorpion, to detect mutations in real-time PCR reactions. All reactions were carried out in 25-μL volumes with 1 μL of template DNA, 7.5 μL of reaction buffer mix, 0.6 μL of primer mix and 0.1 μL of *Taq* polymerase. Real-time PCR was carried out using SmartCycler® II (Cepheid, Sunnyvale, CA, USA) under the following conditions: initial denaturation at 95°C for 10 min, 50 cycles of 95°C for 30 s, and 62°C for 60 s with fluorescence reading (set to FAM that allows optical excitation at 480 nm and measurement at 520 nm) at the end of each cycle. Data analysis was carried out using Cepheid SmartCycler software (version 1.2b). The threshold cycle (Ct) was defined as the cycle at the highest peak of the second derivative curve, which represents the point of maximum curvature of the growth curve. Positive results were defined as Ct 45 and maximum fluorescence intensity 50. Analysis of each sample was carried out in duplicate. The EGFR Scorpion Kit is intended for detection of the two major somatic mutations in *EGFR*. These mutations consist of an in-frame deletion in exon 19 (E746_A750del) and a point mutation in exon 21 (L858R). There are two types of E746_A750del, with starting points at nucleotide positions 2235 and 2236 (NM_005228). The assay can detect both types of E746_A750del. Other deletion patterns in exon 19 and other mutations in the tyrosine kinase domain of EGFR, which are also associated with sensitivity of lung cancers to gefitinib, can not be detected using this assay.

Experiments comparing the detection of E746_A750del in mixtures of wild-type and E746_A750del DNA by direct sequencing and Scorpion ARMS

We used the standard DNA included in the EGFR Scorpion Kit to confirm sensitivity for the detection of E746_A750del. The following DNA mixtures were prepared: 10, 100, 1000 and 10 000 pg E746_A750del DNA, and 10 000 pg wild-type DNA with 10, 100, 1000 and 10 000 pg E746_A750del DNA. These DNA mixtures were used to evaluate the sensitivity of direct sequencing and Scorpion ARMS. The results obtained using Scorpion ARMS were quantified using a standard curve generated by plotting the Ct against the log of the amount of DNA contained in the known standards. The linear correlation coefficient (R^2) values and the formulas for the slopes were calculated. To validate this assay we carried out the assay using plasmid DNA derived from the PCR products of A431 cells, which are known to contain wild-type DNA, PC-9 cells, which are known to contain E746_A750del, and 11-18 cells, which are known to contain L858R. The plasmid DNA was subcloned into a cloning Topo® vector (Invitrogen, Carlsbad, CA, USA). The experiments were carried out at a copy number of 10^7.

Results

Patients and pleural effusion specimens

Twenty-four patients with NSCLC were enrolled in the present study (Table 1). There were 11 women (45.8%) and 10 never-smokers (41.7%). The histological diagnosis was adenocarcinoma in 23 patients and unclassified NSCLC in the other patient. NSCLC was diagnosed cytologically in the pleural effusion samples in 22 of the patients. There were no malignant cells in the pleural effusion fluid of the other two patients. The age range was 39–82 years (median 62 years). Seven patients were treated with gefitinib (250 mg/day) and their response was evaluated. The volume of the pleural effusion fluid collected from the patients ranged from 30 to 280 mL. DNA from cell pellets was extracted for all 24 samples at concentrations ranging from 3.2 to 335.5 ng/μL.

Table 1. Patient characteristics and epidermal growth factor receptor mutation status

No.	Age (years)	Sex	Smoking history	Histology	Response to gefitinib	EGFR mutation	
						Direct sequencing	Scorpion ARMS
1	62	F	Never	ADC	PR	Wild type	E746_A750del
2	40	F	Never	ADC	SD	Wild type	Wild type
3	39	F	Never	ADC	PD	Wild type	Wild type
4	69	M	Former	ADC	–	Wild type	Wild type
5	72	F	Never	ADC	–	Wild type	Wild type
6	66	F	Never	ADC	–	Wild type	Wild type
7	56	M	Current	ADC	–	Wild type	Wild type
8	61	M	Former	ADC	–	Wild type	Wild type
9	65	M	Former	ADC	PD	Wild type	Wild type
10	80	F	Never	ADC	–	Wild type	E746_A750del
11	82	M	Current	NSCLC	–	Wild type	Wild type
12	57	F	Former	ADC	–	Wild type	Wild type
13	55	M	Former	ADC	–	Wild type	Wild type
14	67	M	Former	ADC	–	Wild type	Wild type
15	61	M	Never	ADC	PR	Wild type	E746_A750del
16	65	M	Former	ADC	PR	E746_A750del†	E746_A750del
17	65	F	Former	ADC	–	Wild type	L858R
18	48	F	Never	ADC	–	Wild type	L858R
19	61	M	Current	ADC	–	Wild type	Wild type
20	60	M	Current	ADC	PR	E746_A750del‡	E746_A750del
21	63	F	Never	ADC	–	E746_A750del‡	E746_A750del
22	54	M	Former	ADC	–	Wild type	Wild type
23	49	M	Current	ADC	–	Wild type	Wild type
24	66	F	Never	ADC	–	Wild type	Wild type

Type of mutation: †2236–2250del; ‡2235–2249del (NM_005228). –, Patient did not receive gefitinib; ADC, adenocarcinoma; NSCLC, non-small cell lung cancer; PD, progressive disease; PR, partial response; SD, stable disease.

Sensitivity of direct sequencing and EGFR Scorpion for detection of E746_A740del

Preliminary experiments were carried out to evaluate the sensitivities of direct sequencing and the EGFR Scorpion Kit. When direct sequencing was used to detect E746_A750del in the standard E746_A750del DNA samples (10–10 000 pg), the mutation was detected at amounts as low as 10 pg. When diluted standard E746_A750del DNA was mixed with standard wild-type DNA at ratios from 1:1 to 1:1000, E746_A750del was detected by direct sequencing at ratios as low as 1:10.

When E746_A750del DNA was detected with Scorpion ARMS, all curves for standard E746_A750del DNA (10–10 000 pg) and the primer set for detection of E746_A750del increased for up to 45 cycles (Fig. 1A). When wild-type standard DNA and distilled water were used as negative controls, the curves did not increase, and remained flat at 50 cycles (Fig. 1A). When diluted standard E746_A750del DNA was mixed with wild-type DNA in ratios from 1:1 to 1:1000, all curves that indicated the presence of E746_A750del increased for up to 45 cycles (Fig. 1B). Standard curves in the range of measured amounts in this study were linear with R^2 values of 0.997 and 0.987. Both slopes of the curves were almost parallel (Fig. 1C). The Ct of diluted standard E746_A750del DNA mixed with wild-type DNA was almost the same as for standard E746_A750del DNA. Although the peak fluorescence levels of diluted standard E746_A750del DNA mixed with wild-type DNA were lower than without the wild-type DNA standard, the presence of E746_A750del was clearly detected at the ratio of 1:1000. Curves of DNA containing E746_A750del at amounts up to 10 pg were unaffected by interfusion of wild-type DNA.

The signals of plasmid DNA derived from the PC-9 cells and 11-8 cells were detected at approximately the same Ct values (E746_A750del, 28.6; L858R, 29.2) and, as expected, when plasmid DNA derived from A431 was used, the curve did not increase and remained flat after 50 cycles (Fig. 1D,E).

Detection of *EGFR* mutations by direct sequencing

EGFR mutations in three of the 24 patients (12.5%) were detected by direct sequencing (Table 1). All three were heterozygous, and E746_A750del was detected in all three of them. Figure 2 shows the wave figures of the nucleotide sequence obtained by direct sequencing of part of exon 19 in two patients (patient no. 10, Fig. 2A; patient no. 21, Fig. 2C). The data for patient no. 10 was judged to represent wild-type *EGFR* (Fig. 2A). That of patient no. 21 showed a mixture of wild-type and 2235–2249del sequences (Fig. 2C).

Mutation analysis using the Scorpion ARMS method

EGFR mutation status in all samples was analyzed using the EGFR Scorpion Kit. As wild-type curves were detected in all patients, we concluded that no sample was too small to be detect by the Scorpion ARMS method and that it would be possible to determine the *EGFR* mutation status based on the results. Curves for an *EGFR* mutation were detected in eight of the 24 patients (33.3%; Table 1). In six of these eight patients, curves indicating the presence of a deletion mutation

doi: 10.1111/j.1349-7006.2006.00216.x

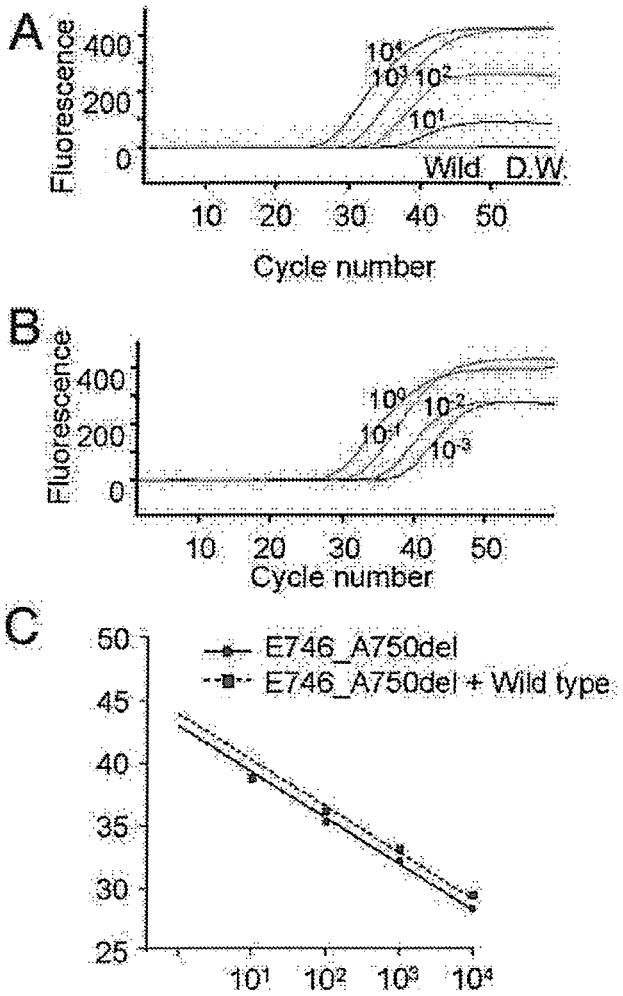

Fig. 1. Sensitivity for detection of the E746_A750del and L858R mutations with the epidermal growth factor receptor (EGFR) Scorpion Kit. (A) Standard E746_A750del DNA was used at various volumes: 10 000 pg (10^4), 1000 pg (10^3), 100 pg (10^2) and 10 pg (10^1). Standard wild-type DNA (Wild) and distilled water (DW), as negative controls, were used in the same experiment. (B) Standard E746_A750del DNA (10–10 000 pg) was mixed with 10 000 pg of standard wild-type DNA at ratios of 1 : 1 (10), 1 : 10 (10^{-1}), 1 : 100 (10^{-2}) and 1 : 1000 (10^{-3}). (C) Standard curves were obtained by plotting the threshold cycle (Ct) of each curve (shown in Fig. 1A,B) against the log of the standard DNA volume. Detection of E746_A750del and L858R in plasmid DNA derived from lung cancer cell lines. (D) PC-9 with E746_A750del DNA and A431 with wild-type DNA. (E) 11-18 with L858R DNA and A431.

in exon 19 were detected (Fig. 2B,D), and curves for the other two patients indicated the presence of L858R in exon 21.

Comparison of detection of the two major mutations by the two methods

In the present study *EGFR* mutations were detected in eight patients. In three of them (nos 16, 20 and 21) the *EGFR* mutations were detected by both methods, whereas in the other five (nos 1, 10, 15, 17 and 18) they were detected by the Scorpion ARMS method alone. No patients were found to have *EGFR* mutations by direct sequencing alone. *EGFR* mutations were not detected using either direct sequencing or the Scorpion ARMS method in two samples that were not diagnosed cytologically as NSCLC.

EGFR mutation status and clinical manifestations

EGFR mutations were detected more frequently in the samples from women (5/11, 45.5% of women; 3/13, 23.1% of men) and non-smokers (5/10, 50.0% of non-smokers; 3/14, 21.4% of smokers) (Table 2). Four of the seven patients who received gefitinib therapy had a partial response, one had stable disease, and the other three patients had progressive disease. All four patients with a partial response had *EGFR* mutations (Table 3). Evaluation of mutation status by the direct sequencing method revealed mutations in two of the four patients with partial response, whereas Scorpion ARMS revealed mutations in all four patients with partial response. Mutation status determined by Scorpion ARMS was superior to mutation status determined

Table 2. Frequency of *epidermal growth factor receptor (EGFR)* mutations in pleural effusion from patients with non-small cell lung cancer according to sex and smoking history

Variable	Direct sequencing		Scorpion ARMS	
	+	−	+	−
Sex and *EGFR* mutant state				
Female	1	10	5	6
Male	2	11	3	10
Smoking history and *EGFR* mutant state				
Non-smoker	1	9	5	5
Smoker	2	13	3	11

+, Mutation positive; −, no mutation; ARMS, Amplified Refractory Mutation System.

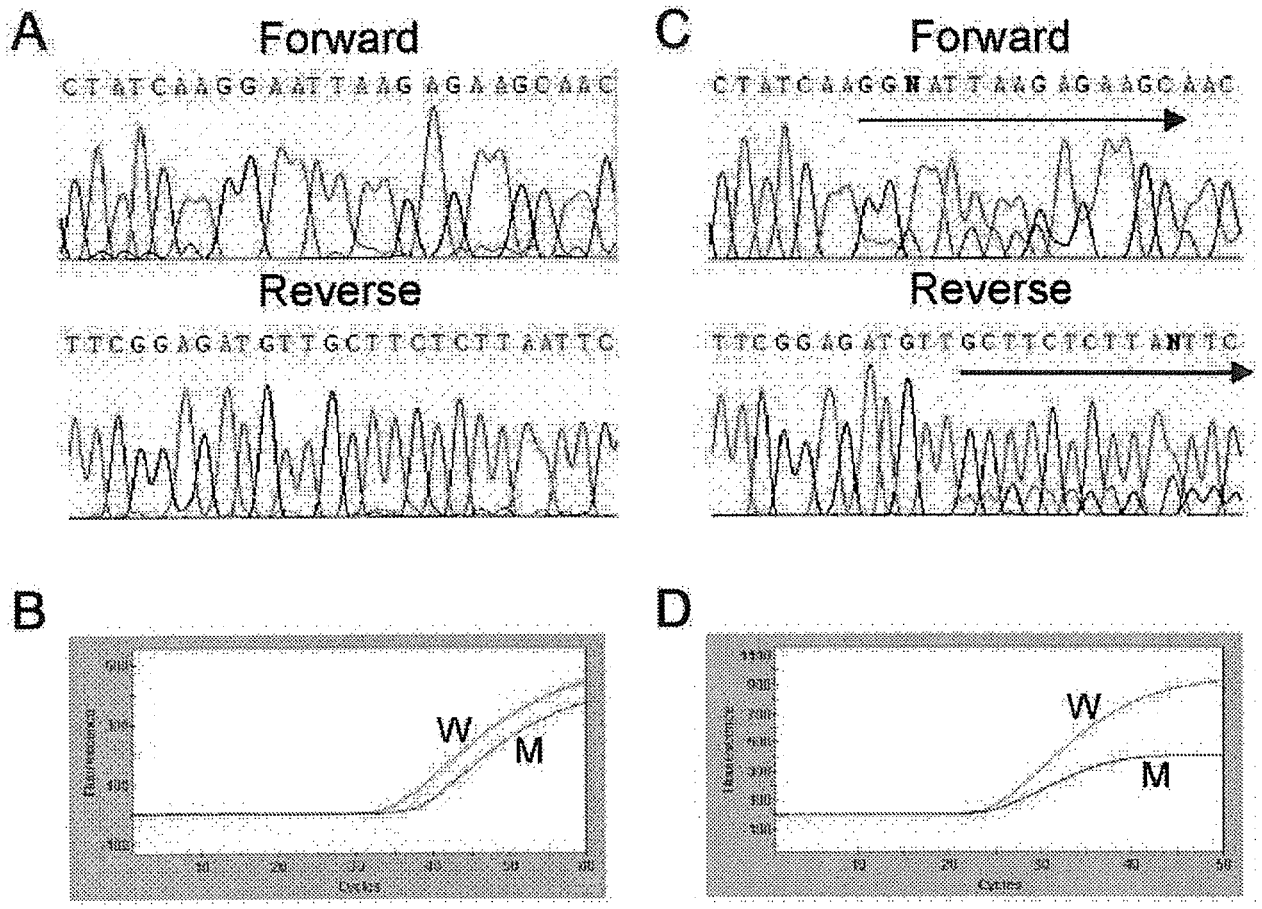

Fig. 2. Results of direct sequencing and the Scorpion Amplified Refractory Mutation System (ARMS) method in patient no. 10 (A,B) and patient no. 21 (C,D). (A) The wave figure represents wild-type *epidermal growth factor receptor (EGFR)*. (B) Two ascending curves, indicating that wild type and deletion mutation in exon 19 were detected. (C) The two waves start to overlap at the starting points of the arrows. These features mean that the nucleotide sequence of the *EGFR* gene in this patient has a heterozygous deletion. The deletion removed amino acids 746–750 (E746_A750del). (D) Two ascending curves, indicating that wild type and deletion mutation in exon 19 were detected.

Table 3. Frequency of *epidermal growth factor receptor (EGFR)* mutations in pleural effusion from patients with non-small cell lung cancer according to response to gefitinib

Variable	Direct sequencing		Scorpion ARMS	
	+	−	+	−
Partial response	2	2	4	0
Stable/progressive disease	0	3	0	3

The response to gefitinib was evaluated in all seven patients treated with gefitinib. +, Mutation positive; −, no mutation.

by direct sequencing for predicting responsiveness to gefitinib. No EGFR mutations were detected in patients with stable disease or progressive disease.

Discussion

The present study yielded two major findings. The first is that *EGFR* mutations, especially E746_A750 del and L858R, were detected in DNA from pleural effusion fluids, and the second is that the Scorpion ARMS method may be more sensitive for detecting *EGFR* mutations than the direct sequencing method. Patients with *EGFR* mutations may be misdiagnosed as not having any mutations if direct sequencing alone is used. Three patients were concluded to have mutations using both methods, but the other four patients were concluded to have mutations by the Scorpion ARMS method alone. As all four of these patients had partial responses to gefitinib, the results strongly suggest a correlation between mutation status and clinical responsiveness to gefitinib, although further clinical study is needed to make a definite conclusion. *EGFR* mutation status determined by the Scorpion ARMS method reflected responsiveness to gefitinib more accurately than direct sequencing.

Direct sequencing is currently the routine method used to detect *EGFR* mutations in tumor samples, and no standard method of detection of *EGFR* mutations in tumor specimens except surgical tissues has been established. The results of our small study lead us to conclude that the EGFR Scorpion Kit is superior to direct sequencing for detection of *EGFR*

doi: 10.1111/j.1349-7006.2006.00216.x

mutations, especially the two major mutations (deletion mutations in exon 19 and L858R), as predictive markers. As our preliminary experiment showed that the sensitivity of Scorpion ARMS for detection of *EGFR* mutations is superior to the sensitivity of direct sequencing when a mixture of wild-type and mutant DNA is used, we infer from these results that the differences in sensitivity for detection in the four patients with the mutations were attributable to the density of tumor cells in the pleural effusion fluid.

To our knowledge detection of *EGFR* mutations in pleural effusion fluid has been described in one case report where the patient responded to gefitinib.[15] Although our study did not confirm a correlation between mutation status and clinical responsiveness to EGFR tyrosine kinase inhibitors such as gefitinib, their results and our own in patients who received gefitinib therapy encourage us to conclude that *EGFR* mutation status determined in pleural effusion fluid may be useful for predicting responsiveness to EGFR tyrosine kinase inhibitors. The authors of the case report did not mention the possibility that normal cells may have prevented detection of *EGFR* mutations in tumor cells and that a patient with an *EGFR* mutation may be concluded not to have a mutation (false negative) as a result.

Some investigators have tried to increase the sensitivity of *EGFR* mutant detection. One attempt involved detection of *EGFR* mutations using a LightCycler PCR assay.[16] SSCP assay is more sensitive than direct sequencing and is a more rapid method.[17] Recently, two rapid and sensitive methods have been demonstrated: the peptide nucleic acid-locked nucleic acid PCR clamp method,[18] and the mutant-enriched PCR assay.[19] In these previous studies, *EGFR* mutations were detected in the presence of 1000-fold and 2000-fold wild-type *EGFR*, respectively. Although the minimum detectable mutation volumes were not evaluated, the sensitivity of these methods seems to be comparable with that of the Scorpion ARMS method, and the sensitivity of these assays seems to be sufficient for clinical use. The latter study used various clinical samples, including 20 samples of pleural fluid. We have shown a relationship between *EGFR* mutation status in pleural fluids and the gefitinib response in a portion of the enrolled patients. The relationship in the remaining patients is currently being evaluated, and confirmation is expected in the very near future. As the Scorpion ARMS method is simple and very fast, it may be suitable for mutation screening. However, one limitation of the EGFR Scorpion Kit is that it is only able to detect mutations targeted by the Scorpion primers. It is known that deletion mutations in exon 19 have many variations in deleted nucleotides and addition of point mutations. The Scorpion ARMS method could detect mutations targeted by primers designed in advance and is capable of detecting the specific mutation E746_A750del in exon 19. E747_P753del insS and L747_T751del are minor variations of deletion mutations in exon 19 and could not be detected using this method in another study (data not shown). All *EGFR* mutations are not at these two sites; some are clustered around the ATP-binding site in exons 18, 19 and 21.[3–8] Although approximately 90% of NSCLC-associated *EGFR* mutations consist of the two major EGFR mutations,[5,8] other mutations may be misdiagnosed as negative mutation results using the Scorpion ARMS method. Moreover, a secondary mutation, a substitution of methionine for threonine at position 790 (T790M), leads to gefitinib resistance in NSCLC patients who have *EGFR* mutations and are responsive to gefitinib.[20,21] These mutation states may also be critical factors for gefitinib therapy. Scorpion primers need to be designed to detect these mutations, and further study using these primers is required.

Our two initial aims, which were to detect two major EGFR mutations in pleural effusion fluid and to increase the sensitivity of detection of *EGFR* mutations in the mixtures of DNA from normal cells and tumor cells, were achieved in this study. As the next step, a prospective study of a large number of NSCLC patients with pleural effusion is likely to reveal a correlation between *EGFR* mutation state in pleural effusion fluids and clinical responsiveness to EGFR tyrosine kinase inhibitors, such as gefitinib.

Acknowledgments

We wish to thank Dr Stephan Little (Dxs, Manchester, UK) for providing the EGFR Scorpion Kit and technical assistance. H. Kimura received support from an awardee of a Research Resident Fellowship from the Foundation for Promotion of Cancer Research (Japan) for the 3rd Term Comprehensive 10-Year Strategy for Cancer Control.

References

1 Parkin DM, Bray F, Ferlay J, Pisani P. Global cancer statistics, 2002. *CA Cancer J Clin* 2005; **55**: 74–108.
2 Franklin WA, Veve R, Hirsch FR *et al.* Epidermal growth factor receptor family in lung cancer and premalignancy. *Semin Oncol* 2002; **29**: 3–4.
3 Lynch TJ, Bell DW, Sordella R *et al.* Activating mutations in the epidermal growth factor receptor underlying responsiveness of non-small-cell lung cancer to gefitinib. *N Engl J Med* 2004; **350**: 2129–39.
4 Paez JG, Janne PA, Lee JC *et al.* EGFR mutations in lung cancer: correlation with clinical response to gefitinib therapy. *Science* 2004; **304**: 1497–500.
5 Pao W, MillerV, Zakowski M *et al.* EGF receptor gene mutations are common in lung cancers from 'never smokers' and are associated with sensitivity of tumors to gefitinib and erlotinib. *Proc Natl Acad Sci USA* 2004; **101**: 13 306–11.
6 Shigematsu H, Lin L, Takahashi T *et al.* Clinical and biological features associated with epidermal growth factor receptor gene mutations in lung cancers. *J Natl Cancer Inst* 2005; **97**: 339–46.
7 Han SW, Kim TY, Hwang PG *et al.* Predictive and prognostic impact of epidermal growth factor receptor mutation in non-small-cell lung cancer patients treated with gefitinib. *J Clin Oncol* 2005; **23**: 2493–501.
8 Kosaka T, Yatabe Y, Endoh H *et al.* Mutations of the epidermal growth factor receptor gene in lung cancer: biological and clinical implications. *Cancer Res* 2004; **64**: 8919–23.
9 Pass HI, Carbone DP, Johnson DH *et al. Lung Cancer Principles and Practice*, 3rd edn. Philadelphia: Lippincott, Williams & Wilkins 2005; 291–303.
10 Fenton KN, David Richardson J. Diagnosis and management of malignant pleural effusions. *Am J Surg* 1995; **170**: 69–74.
11 Whitcombe D, Theaker J, Guy SP *et al.* Detection of PCR products using self-probing amplicons and fluorescence. *Nat Biotechnol* 1999; **17**: 804–7.
12 Newton CR, Graham A, Heptinstall LE *et al.* Analysis of any point mutation in DNA. The amplification refractory mutation system (ARMS). *Nucl Acids Res* 1989; **17**: 2503–16.
13 Wookey A, Ellison G, Donald E *et al.* Comparison of methods for the detection of mutations in the epidermal growth factor receptor gene. *Ann Meeting Am Assoc Cancer Res* 2005; **96**: 5287. [Abstract]
14 Therasse P, Arbuck SG, Eisenhauer EA *et al.* New guidelines to evaluate the response to treatment in solid tumors. European Organization for Research

and Treatment of Cancer, National Cancer Institute of the United States, National Cancer Institute of Canada. *J Natl Cancer Inst* 2000; **92**: 205–16.
15 Huang MJ, Lim KH, Tzen CY *et al.* EGFR mutations in malignant pleural effusion of non-small cell lung cancer: a case report. *Lung Cancer* 2005; **49**: 413–15.
16 Sasaki H, Endo K, Konishi A *et al.* EGFR mutation status in Japanese lung cancer patients: genotyping analysis using LightCycler. *Clin Cancer Res* 2005; **11**: 2924–9.
17 Marchetti A, Martella C, Felicioni L *et al.* EGFR mutations in non-small-cell lung cancer: analysis of a large series of cases and development of a rapid and sensitive method for diagnostic screening with potential implications on pharmacologic treatment. *J Clin Oncol* 2005; **23**: 857–65.
18 Nagai Y, Miyazawa H, Huqun *et al.* Genetic heterogeneity of the epidermal growth factor receptor in non-small cell lung cancer cell lines revealed by a rapid and sensitive detection system, the peptide nucleic acid-locked nucleic acid PCR clamp. *Cancer Res* 2005; **65**: 7276–82.
19 Asano H, Toyooka S, Tokumo M *et al.* Detection of EGFR gene mutation in lung cancer by mutant-enriched polymerase chain reaction assay. *Clin Cancer Res* 2006; **12**: 43–8.
20 Kobayashi S, Boggon TJ, Dayaram T *et al.* EGFR mutation and resistance of non-small-cell lung cancer to gefitinib. *N Engl J Med* 2005; **352**: 786–92.
21 Kwak EL, Sordella R, Bell DW *et al.* Irreversible inhibitors of the EGF receptor may circumvent acquired resistance to gefitinib. *Proc Natl Acad Sci USA* 2005; **102**: 7665–70.

doi: 10.1111/j.1349-7006.2006.00216.x

The FASEB Journal express article 10.1096/fj.05-4034fje. Published online December 22, 2005.

Dimerization and the signal transduction pathway of a small in-frame deletion in the epidermal growth factor receptor

Kazuko Sakai,*,§ Tokuzo Arao,* Tatsu Shimoyama,* Kimiko Murofushi,§ Masaru Sekijima,‖ Naoko Kaji,‖ Tomohide Tamura,† Nagahiro Saijo,† and Kazuto Nishio*,‡

*Shien-Lab, Medical Oncology, and †National Cancer Center Hospital and ‡Pharmacology Division, National Cancer Center Research Institute, Tsukiji 5-1-1, Chuo-ku, Tokyo, Japan; and §Department of Biology, Faculty of Science, Ochanomizu University, Tokyo, Japan; and ‖Mitsubishi Chemical Safety Institute, Ibaraki, Japan

Corresponding author: Kazuto Nishio, Shien-Lab, Medical Oncology, National Cancer Center Hospital, Tsukiji 5-1-1, Chuo-ku, Tokyo 104-0045, Japan. E-mail: knishio@gan2.res.ncc.go.jp

ABSTRACT

A short, in-frame deletional mutant (E746-A750del) is one of the major mutant forms of epidermal growth factor receptor (EGFR) and has been reported to be a determinant of response to EGFR tyrosine kinase inhibitors such as gefitinib and erlotinib. However, the biological and pharmacological functions of mutational EGFR remain unclear. To clarify these biological functions of deletional EGFR, we examined the cellular response to EGF ligand stimulation. Dimerization and phosphorylation of EGFR were observed without any ligand stimulation in the 293(D) cells transfected with deletional EGFR as compared with those transfected with wild-type EGFR (293(W) cells). When the 293(D) cells were exposed to gefitinib, an immunoblotting analysis revealed remarkable inhibition of AKT phosphorylation but not phospho-p44/42 MAPK. To examine the cellular response in a lung cancer cell line intrinsically expressing deletional EGFR, phospho-EGFR, and downstream reactions were monitored under EGF stimulation with a beads-based mulitiplex assay. EGFR and its downstream proteins were constitutively phosphorylated in the PC-9 cells without any ligand stimulation as compared with A549 lung cancer cells expressing wild-type EGFR. In conclusion, deletional EGFR is constitutively active and phosphorylates p44/42 MAPK and AKT in the cells, although the fact that the EGFR phosphorylation in the PC-9 cells is still modulated by EGF stimulation cannot be ignored. Gefitinib-inhibited phospho-AKT predominantly in deletional EGFR expressing cells.

Key words: mutation • gefitinib • tyrosine kinase

Epidermal growth factor receptor (EGFR) belongs to the ErbB family (1) and contains an extracellular ligand-binding domain, a transmembrane domain, and a tyrosine kinase domain. Wild-type EGFR is unphosphorylated and exists as a monomer in the unstimulated conditions. Binding of ligands such as EGF and TGF-α leads to the dimerization of EGFR, phosphorylation of tyrosine residues (2), and stimulation of the phosphorylation pathway downstream. This signaling pathway is considered to be closely related to cellular growth, differentiation, and the development of malignant phenotypes of cancer cells (1, 2). Increased

expression of EGFR and gene amplification of EGFR are often observed in several types of tumors such as lung and breast cancers.

Recently, many small anticancer molecules have been developed that target EGFR. Gefitinib (Iressa) is an orally available EGFR tyrosine kinase inhibitor. Previous clinical studies have demonstrated that EGFR expression levels in tumors did not correlate with the clinical response to gefitinib (3). On the other hand, EGFR mutation in adenocarcinoma of the lung was reported to be a determinant of sensitivity for EGFR tyrosine kinase inhibitors such as gefitinib and erlotinib (4, 5). To date, over 30 types of EGFR mutation have been reported in lung cancer. The in-frame, 15 base deletional mutation (delE746-A750 type deletion) is one of the most common of these EGFR mutations. We previously demonstrated that overexpression of deletional EGFR increased the cellular sensitivity to tyrosine kinase inhibitors targeting EGFR in human HEK293 cells in vitro (6). However, it remains unclear how deletional EGFR alters dimerization and the downstream signaling pathways from these heterodimers. Recently, Tracy et al. demonstrated that another major mutant EGFR (L858R) altered signal transduction downstream (7). In addition, it has been suggested that the L858R mutation is a hyper-response to ligand stimulation (7). We hypothesized that the deletional EGFR is constitutively active. The aim of this study was to clarify the downstream of the signaling and its function of the deletional EGFR.

Technically, a beads-based multiplex assay (Bio-Plex phosphoprotein assay) (8) allowed us to analyze numbers of phosphoproteins simultaneously after ligand stimulation.

MATERIALS AND METHODS

Reagents

Gefitinib (Iressa, ZD1839) was provided by AstraZeneca (Cheshire, UK).

Cell culture

The human embryonic kidney HEK293 cell line and human nonsmall-cell lung cancer (NSCLC) cell line A549 and cervix epitheloid cancer cell line HeLa were obtained from the American Type Culture Collection (Manassas, VA) and were cultured in RPMI 1640 medium supplemented with 10% FBS. The human NSCLC cell line PC-9 was established at the Tokyo Medical University (9, 10), and was maintained in RPMI 1640 medium (Sigma, St. Louis, MO) supplemented with 10% heat-inactivated fetal bovine serum (FBS; Life Technologies, Rockville, MD).

Plasmid construction and transfection

The construction of the mock expression plasmid vector (empty vector) and of the wild-type of EGFR and the 15-bp deletional EGFR (delE746-A750 type deletion) vectors that posses the same deletion site observed in PC-9 cells has been described in another paper in detail (6, 11, 12). The plasmids were transfected into the HEK293 cells, and the transfectants were selected by Zeosin (Sigma). The stable transfectants (pooled cultures) of the empty vector, wild type of EGFR, and its deletion mutant were designated as 293(M), 293(W), and 293 (D) cells, respectively.

Reverse-transcription PCR

Five micrograms of total RNA from each cultured cell line was converted to cDNA with a GeneAmp RNA-PCR kit (Applied Biosystems, Foster City, CA). The primers used for the PCR were EGFR (forward), 5′-AAGTTAAAATTCCCGTCGCTATCA-3′ and (reverse) 5′-GAGCCAATATTGTCTTTGTGTTCC-3′. PCR amplification consisted of 28 cycles (95°C for 45 s, 57.5°C for 30 s, and 72°C for 45 s) followed by incubation at 72°C for 7 min. The RT-PCR products were analyzed with a 2100 Bioanalyzer and DNA 500 kit (Agilent Technologies, Waldbronn, Germany).

Chemical cross-linking

After treatment with or without EGF (Sigma), monolayer cells were washed twice with ice-cold phosphate buffered saline containing 0.33 mM $MgCl_2$ and 0.9 mM $CaCl_2$ (PBS(+)) and chemically cross-linked for 20 min at room temperature with freshly prepared 1.5 mM bis(sulfosuccinimidyl) suberate (BS^3, Pierce, Rockford, IL). To terminate the reaction, a final concentration of 20 mM glycine was added for an additional 5 min. For immunoblot analysis, the cells were washed twice with ice-cold PBS(+) and lysed with M-PER mammalian protein extraction reagent (Pierce). The lysate was centrifuged at 20,000 *g* for 10 min, and the protein concentration of the supernatant was measured with a BCA (bicinchoninic acid) protein assay (Pierce).

Ligand stimulation

After reaching 70–80% confluence, cultured cells were stimulated with EGF, TGF-α, and HB-EGF for 10 min under nonstarved conditions or serum-starved conditions. The cells were washed twice with ice-cold PBS(+), and lysed for immunoblotting.

Drug treatment

After reaching 70–80% confluence, cultured cells, were exposed to various concentrations of gefitinib and stimulated or not stimulated with EGF (100 ng/ml) for 10 min under nonstarved conditions or serum-starved conditions. The cells were washed twice with ice-cold PBS(+) and lysed for immunoblotting.

Immunoblot analysis

Immunoblot analysis was performed as described previously (12). Equivalent amounts of protein were separated by electrophoresis on a SDS-PAGE and transferred to a polyvinylidene difluoride (PVDF) membrane (Millipore, Bedford, MA). The membrane was probed with a mouse monoclonal antibody against EGFR (Transduction Lab, San Diego, CA), a phospho-EGFR antibody (specific for Tyr1068), p44/42 mitogen-activated protein kinase (p44/42 MAPK), phospho-p44/42 MAPK, AKT, phospho-AKT, nuclear factor-κB (NF-κB) inhibitor α (IκB-α), and phospho-IκB-α antibody (Cell Signaling Technology, Beverly, MA) as the first antibody, followed by a horseradish peroxidase-conjugated secondary antibody. The bands were visualized with electrochemiluminescence (ECL, Amersham, Piscataway, NJ), and images of blotted patterns were analyzed with NIH image software (National Institutes of Health, Bethesda, MD).

Phosphoprotein assay

A panel of phosphoproteins was measured in duplicate using a bead-based mulitiplex assay (Bio-Plex phosphoprotein assay, Bio-Rad, Hercules, CA), according to the manufacturer's instructions (8, 13). The EGFR-transfected 293 cells and NSCLC cells cultured in the serum-free medium for 24 h were stimulated by the addition of EGF at a final concentration of 100 ng/ml for the indicated time intervals. After incubation, the cells were rinsed with ice-cold Cell Wash Buffer and collected. The lysate was centrifuged at 1,700 *g* for 20 min. The protein concentration was calculated with a DC (detergent compatible) protein assay (Bio-Rad). The Bio-Plex assay was customized to detect and quantify phosphoproteins of EGFR, p44/42 MAPK, activating transcription factor 2 (ATF-2), c-Jun N-terminal kinase (JNK), p38 mitogen-activated protein kinase (p38 MAPK), IκB-α, and signal transducer and activator of transcription 3 (STAT-3). The prepared first antibody with coupled beads was captured under 96-well plates, and samples (17.5 μg each) were incubated overnight at room temperature. Samples were incubated with biotin-labeled detection antibodies followed by further incubation with the fluorescence-labeled avidin reporter. The level of phosphoproteins bound to the beads was indicated by the intensity of the reporter signal. The signal was measured with Bio-Plex Manager software (Bio-Rad) interfaced with a Bio-Plex Reader (Bio-Rad). In this assay, we used the lysates of untreated HeLa cells as the background control for all phosphoprotein assays provided by the Bio-Plex phosphoprotein assay (14). This experiment was repeated in duplicate.

RESULTS

Dimerization and phosphorylation of wild-type EGFR and deletional EGFR

The EGFR expression level in the 293 cells transfected with the empty vector (293(M)), wild-type EGFR (293(W)), and deletional EGFR (293(D)), in the A549 and PC-9 NSCLC cells, and in the HeLa cervix epitheloid cancer cells were determined by RT-PCR and immunoblot analysis (Fig. 1). The PCR products were separated into wild-type EGFR (upper band) and deletion mutant EGFR (lower band) by the different lengths of the sequences. Overexpression of EGFR was detected in the 293(W) and 293(D) cells. Only a small amount of intrinsically EGFR was detected in 293(M) cells by RT-PCR. We sequenced exon 19 and 20 of EGFR in HEK293 cells, but no mutations were detected (data not shown). A high level of EGFR expression was detected in the PC-9 cells, and a moderate level was detected in the A549 and HeLa cells. The EGFR protein levels closely matched the mRNA expression levels in all cells.

Dimerization of EGFR, the first step in the EGFR signaling pathway, was examined by chemical cross-linking. The 293(M), 293(W), and 293(D) cells were treated with EGF (10 ng/ml) for 10 min under nonstarved conditions (Fig. 2*A*). Cells were incubated with the cross-linking reagent BS^3. Dimerization and phosphorylation of EGFR were determined by immunoblot with anti-EGFR and anti-phospho EGFR antibodies. Dimerization and expression of EGFR were not detected in the 293(M) cells. Dimerized EGFR with a molecular weight of ~400 kDa was detected in the 293(W) cells. Increased phosphorylation and dimerization of the deletional EGFR were detected without EGF stimulation in the 293(D) cells by the chemical cross-linking and immunoblot assay, respectively. When the cells were stimulated with the EGF ligand (10 ng/ml for 10 min), increased phospho-EGFR dimers were observed in the 293(W) cells, whereas no response of EGFR to EGF was observed in the 293(D) cells. We quantified the levels of monomeric and dimerized EGFR in the 293(W) and 293(D) cells densitometrically under nonstarved conditions (Fig. 2*A*, right). In the

293(W) cells, the dimer/monomer ratio was increased ~40% by the addition of EGF. Addition of EGF slightly increased the dimer/monomer ratio (~20%) in the 293(D) cells.

We investigated the dimerization and phosphorylation status of EGFR in the EGFR-transfected cell lines under serum-starved conditions (Fig. 2*B*). The transfected cells were exposed by EGF (10 ng/ml for 10 min) after serum starvation for 24 h. No expression of EGFR dimer or monomer was detected in the 293(M) cells. Addition of EGF resulted in an increase in dimerized and phosphorylated EGFR in the 293(W) cells. Dimerization and phosphorylation of the deletional EGFR were detected in the 293(D) cells in the absence of EGF after serum starvation. Expression of dimerized EGFR in the 293(D) cells was unchanged by EGF stimulation. These findings demonstrated that the deletional mutant EGFR was constitutively dimerized and phosphorylated without any ligand stimulation even under starved conditions and are consistent with the results under nonstarved conditions (Fig. 2*A*). The ratio of dimerized to monomeric EGFR in 293(W) and 293(D) cells was analyzed densitometrically under serum-starved conditions (Fig. 2*B*, right). The dimer/monomer ratio in the 293(W) cells was markedly increased (~3 fold) by addition of EGF. Under unstimulated conditions, the dimer/monomer ratio of the 293(D) cells was higher than that of the 293(W) cells, and the ratio was unchanged by addition of EGF.

These results suggest that the cells expressing the wild-type of EGFR responded to EGF for their dimerization and phosphorylation and that the deletion mutant of EGFR was dimerized and phosphorylated constitutively without any ligand stimulation.

Phosphorylation of EGFR, p44/42 MAPK, and AKT in the EGFR-transfected 293 cells

The p44/42 MAPK and AKT are major downstream targets of EGFR. We examined the phosphorylation status of p44/42 MAPK and AKT with EGF addition in the transfectants. The transfected cells were treated with EGF (10 ng/ml) for 10 min under nonstarved conditions (Fig. 3*A*). The phosphorylation levels of EGFR in the 293(D) cells were higher without any ligand stimulation than that of the 293(W) cells. Phospho-EGFR in the 293(W) cells was increased after EGF stimulation. These findings are consistent with Fig. 2. Even under unstimulated conditions, increased phosphorylation of p44/42 MAPK and AKT was observed in the 293(D) cells. In the 293(W) cells, increased phosphorylation of p44/42 MAPK and AKT was observed with the addition of EGF especially p44/42 MAPK was remarkably phosphorylated. On the other hand, in the 293(D) cells, phosphorylation of p44/42 MAPK and AKT was not increased with the addition of EGF. We quantified the phosphorylation levels of p44/42 MAPK and AKT densitometrically in the transfectants in response to EGF. The addition of EGF increased phosphorylation of p44/42 MAPK in the 293(M) cells (~3.4 fold) and in the 293(W) cells (~2.5 fold) (Fig. 3*B*), suggesting no difference in response in regard to p44/42 MAPK to EGF. Increased phosphorylation of AKT in the 293(M) cells (~2.1 fold) and in the 293(W) cells (~1.3 fold) was observed. By contrast, EGF decreased the phosphorylation of p44/42 MAPK and AKT in the 293(D) cells ~30% and ~20% (Fig. 3*C*). These findings suggest that the p44/42 MAPK and AKT pathways are activated in cells expressing the deletional EGFR without ligand stimulation.

Next, we examined the dose-dependent response of EGFR status in the transfected cells to the other ligands, TGF-α, and HB-EGF, after serum starvation (Fig. 4). The hyperphosphorylated EGFR in the 293(D) cells was unchanged by stimulation with these ligands either. By contrast, a dose-dependent increase in EGFR phosphorylation was observed in the 293(W) cells in response to stimulation by TGF-α and HB-EGF. Both HB-EGF and EGF strongly increased EGFR

phosphorylation in the 293(W) cells compared with TGF-α. We also examined the downstream in response to these ligands. In the 293(W) cells, increased phosphorylation of p44/42 MAPK and AKT was observed in response to addition of the ligands (EGF, TGF-α, and HB-EGF). p44/42 MAPK was markedly phosphorylated by the ligands. In the 293(D) cells, addition of ligands further increased p44/42 MAPK phosphorylation. The AKT phosphorylation in the 293(D) cells was unchanged by stimulation with these ligands. These findings are consistent with the data in Fig. 3*A*, and suggest that the p44/42 MAPK and AKT pathways are both activated in cells constitutively expressing the deletional EGFR.

Effect of gefitinib on phosphorylation of EGFR, p44/42 MAPK, and AKT in the EGFR-transfected 293 cells

Previously, we demonstrated that 293(D) cells were hypersensitive to EGFR-targeted tyrosine kinase inhibitors such as gefitinib and ZD6474, as compared with 293(W) cells (6). To examine the specific action of these tyrosine kinase inhibitors on deletional EGFR signal transduction, we exposed the 293 transfectants to gefitinib, and its cellular response was examined under nonstarved conditions with an immunoblot analysis (Fig. 5*A*). In the 293(W) cells, phosphorylation of p44/42 MAPK was not inhibited by exposure to a low dose of gefitinib (0.01 μM) but phosphorylation of AKT was inhibited by exposure to gefitinib (0.01 μM). In contrast, exposure to gefitinib decreased phospho-EGFR in the 293(D) cells that are hypersensitive to gefitinib. Phosphorylation of AKT was completely inhibited by 0.01 μM gefitinib exposure, while the inhibition of p44/42 MAPK phosphorylation was not remarkable in the 293(D) cells. The effect of 0.01 μM gefitinib on phosphorylated p44/42 MAPK and AKT in the transfectents measured densitometrically. p44/42 MAPK phosphorylation in the 293(M) and 293(W) cells was unaltered by gefitinib exposure for 3 h, but it decreased in the 293(D) cells (~20%) (Fig. 5*B*). Gefitinib increased phosphorylation of AKT ~1.3 fold in the 293(M) cells. Gefitinib inhibited AKT phosphorylation was ~70% in the 293(W) cells, and decreased it ~99% in the 293(D) cells (Fig. 5*C*).

We examined the dose-dependent effect of gefitinib (0.02, 0.2, 2 μM) on EGFR and its downstream signaling in all of the transfectants under serum-starved conditions. Phosphorylation of EGFR was not detected in the 293(W) cells under the 24 h serum-starved conditions, and gefitinib had no effect on it (Fig. 6*A*). Hyperphosphorylation of EGFR was dose dependently inhibited by gefitinib in the 293(D) cells. p44/42 MAPK and AKT were slightly phosphorylated in the 293(W) cells, and their degree of phosphorylation was unaltered by exposure to gefitinib. By contrast, gefitinib dose-dependently decreased phosphorylation of p44/42 MAPK, and AKT in the 293(D) cells. Under EGF stimulation (Fig. 6*B*), gefitinib dose-dependently decreased phosphorylation of EGFR, p44/42 MAPK, and AKT in the 293(W) cells. Phosphorylation of EGFR in the 293(D) cells was completely inhibited by a low concentration of gefitinib (0.02 μM), and phosphorylation of p44/42 MAPK and AKT was dose-dependently inhibited by gefitinib. A low concentration of gefitinib inhibited EGFR phosphorylation and its signal in the 293(D) cells under serum-starved conditions. The phosphorylation of EGFR (and its signal) induced by EGF-addition in the 293(W) cells was inhibited by gefitinib dose dependently.

These data suggest that gefitinib inhibited the AKT signaling pathway more strongly than the p44/42 MAPK signaling pathway in the cells expressing the deletional mutant EGFR.

Response to EGF stimulation in the EGFR-transfected 293 cells

We performed the quantitative phosphoprotein analysis in the 293(W) and 293(D) cells by a beads-based multiplex assay. Downstream from the reaction, we monitored the phosphorylation status of p44/42 MAPK, JNK, and p38 MAPK. We also examined the phosphorylation status of ATF-2 that is located downstream of the MAPK pathway, IκB-α that is a member of the AKT pathway, and STAT-3 that is found downstream of the other signaling pathway. Even under unstimulated conditions, EGFR was hyperphosphorylated in the 293(D) cells but not in the 293(W) cells (Fig. 7*A*). Increased phosphorylation of EGFR was observed in the 293(W) cells (~40 fold), but the phosphorylation of EGFR in the 293(W) cells was much lower than that of the deletional EGFR in the 293(D) cells. IκB-α phosphorylation in the transfected cells was as low as in the HeLa cells, which was used as a negative control (Fig. 7*B*). Under unstimulated conditions, phosphorylation of p44/42 MAPK was greater in the 293(D) cells than in the 293(W) cells (~3 fold) (Fig. 7*C*). A large increase in phosphorylation of p44/42 MAPK in response to the addition of EGF was observed in the 293(W) cells (~15 fold), and a smaller increase was observed in the 293(D) cells (~3.5 fold). These differences in phosphorylated p44/42 MAPK in the 293(W) and 293(D) cells detected in the beads-based multiplex assay are consistent with the result of immunoblotting (Fig. 4). ATF-2 was phosphorylated in the 293(W) cells (~1.5 fold) and 293(D) cells (~1.7 fold) by addition of EGF (Fig. 7*D*). By contrast, the JNK in the 293(W) cells was phosphorylated by addition of EGF (~2 fold), but not phosphorylated in the 293(D) cells (Fig. 7*E*). Phosphorylation of p38 MAPK and STAT-3 was not detected in either type of cell (data not shown). These findings suggest that the p44/42 MAPK and AKT pathways are both phosphorylated without any ligand stimulation in the cells expressing the deletional mutant EGFR.

Response to EGF stimulation in PC-9 cells intrinsically expressing deletional EGFR

The hyperphosphorylation and increased dimerization of deletional EGFR has been demonstrated by ectopic expression of deletional EGFR. To examine whether this phenomenon is also observed in the lung cancer cells intrinsically expressing deletional EGFR, we monitored the phosphorylation of EGFR and its related molecules in the PC-9 cells as compared with the A549 cells. The PC-9 cells and A549 cells express the deletional and wild-type EGFR, respectively. PC-9 cells also express a small amount of wild-type EGFR, and so these cell lines mimic the 293(D) cells. We examined the phosphorylation of EGFR and its downstream signaling molecules in these cells by immunoblotting (Fig. 8*A*). Increased phosphorylation of EGFR was observed in the PC-9 cells even under unstimulated conditions, but not in the A549 cells. The addition of EGF markedly increased the EGFR phosphorylation in the A549 cells compared with the PC-9 cells. Under unstimulated conditions, p44/42 MAPK, and AKT were more phosphorylated in the PC-9 cells than in the A549 cells. Increased phosphorylation of p44/42 MAPK and AKT was observed in the A549 cells after addition of EGF, and p44/42 MAPK was markedly phosphorylated. A small increase in phosphorylation of p44/42 MAPK and AKT was observed in the PC-9 cells in response to the addition of EGF. The increased phosphorylation of IκB-α in the PC-9 cells was observed even under unstimulated conditions. The addition of EGF increased the phosphorylation of IκB-α in the A549 cells but did not alter it in the PC-9 cells. These findings suggest a difference in reactivity to the EGF stimulation between the A549 and PC-9 cells.

Next, examination was performed by a beads-based mulitiplex assay. Increased phosphorylation of EGFR was observed in the PC-9 cells, even under unstimulated conditions, but not in the A549 cells (Fig. 8*B*). These findings are consistent with the results of immunoblotting. EGFR

phosphorylation was markedly increased in the A549 cells (~100-fold), and to a lesser extent increased in the PC-9 cells (~1.4-fold). IκB-α was phosphorylated in the PC-9 cells in the absence of EGF stimulation (Fig. 8*C*), suggesting that the AKT pathway, including IκB-α, was activated in the PC-9 cells expressing deletional EGFR, compared with A549 cells. p44/42 MAPK and ATF-2 were phosphorylated without EGF stimulation in the PC-9 cells compared with the A549 cells (Fig. 8*D* and *E*). A large increase in phosphorylation of p44/42 MAPK and ATF-2 was observed in the A549 cells (~13 fold and ~4.3 fold), and a smaller increase was observed in the PC-9 cells (~3.5-fold and ~1.7-fold). JNK was not phosphorylated in either the A549 or the PC-9 cells. Phosphorylation of JNK in response to EGF stimulation was detected in the A549 cells (~2.6-fold), but not in the PC-9 cells (Fig. 8*F*). No phosphorylation of p38 MAPK and STAT-3 was detected in either cell line (data not shown). These differences in phosphoproteins in the A549 and PC-9 cells are consistent with the results of the beads-based multiplex assay in the EGFR-transfected cells (293(W) and 293(D)) (Fig. 7).

To determine whether there was a significant difference between unstimulated and EGF-stimulated conditions, a statistical analysis was performed using the *t* test. There were significant differences between increased phospho-EGFR, phospho-p44/42 MAPK, phospho-ATF-2, and phospho-JNK ($P>0.01$) in the A549 cells under unstimulated and EGF-stimulated conditions. There were also significant differences in the increased phospho-EGFR, phospho-p44/42 MAPK, phospho-ATF-2, and phospho-IκB-α ($P>0.01$) in the PC-9 cells. The fact that phosphorylation of EGFR, p44/42 MAPK, and ATF-2 in the PC-9 cells is still modulated by EGF stimulation cannot be ignored. This pathway is considered to be preferentially regulated by wild-type EGFR.

DISCUSSION

Previous studies have demonstrated that mutational EGFR is a major factor against determining gefitinib sensitivity. We analyzed the characteristics of deletional EGFR with cells expressing deletional EGFR.

In Fig. 3, phosphorylation of p44/42 MAPK and AKT was increased by EGF in the 293(M) cells, although the EGFR was not overexpressed in these cells. There is a rich cross-talk among the ErbB family that regulates the cellular effects mediated by these receptors. However, ErbB-2 (HER2), ErbB-3 (HER3), and ErbB-4 (HER4) are not expressed, and intrinsic EGFR was weakly expressed in the 293 cells (15). Activation of p44/42 MAPK and AKT in response to EGF might be mediated by the intrinsic EGFR. On the other hand, constitutive activation of EGFR and its downstream pathway is due to the mutant EGFR in the 293(D) cells, suggesting that the mutant EGFR shows a dominant phenotype.

In Fig. 3, p44/42 MAPK and AKT were activated under unstimulated conditions in the 293(D) cells. In these transfectants, EGF did not enhance the phosphorylation of p44/42 MAPK and AKT in contrast to those in the 293(W) cells. The phosphorylation of AKT in these cells seems to be decreased by the addition of EGF (Fig. 3*A*). It can be speculated that EGF negatively regulated the activation of mutant EGFR as a feedback mechanism. It is uncertain whether EGF itself negatively regulates the mutant EGFR. Although the mechanism of this phenomenon remains uncertain, a feedback mechanism might be postulated as a possible explanation. It was reported that leucine-rich repeats and immunoglobulin-like domains 1 (LIRG1) is a negative regulator of EGFR (16) and its transcription was up-regulated by EGF stimulation and caused consequently

degradation of EGFR. Thus the feedback mechanisms, including that mediated by LIRG1, should be clarified in the future study.

The 293(D) cells transfected with deletional EGFR were hypersensitive to the growth-inhibitory effect of EGFR tyrosine kinase inhibitor, including gefitinib (6). AKT phosphorylation was completely suppressed by 0.01 μM gefitinib in the 293(D) cells (Fig. 5). It is suggested that deletional EGFR signaling inclines toward the AKT pathways, and this is correlated with cellular sensitivity to gefitinib. The response to gefitinib in the 293(M) cells cannot be ignored. We speculate that the difference in cell response to gefitinib may be attributable to cell dependency on EGFR in the 293(M), 293(W), and 293(D) cells. Since the 293(W) and 293(D) cells seem to be largely dependent on EGFR, therefore, gefitinib effectively inhibited the AKT phosphorylation in these cells. Cell growth in 293(M) cells, on the other hand, is regulated by other signaling pathways. Then the MAPK and AKT pathways did not respond to gefitinib. In addition, the PC-9 cells intrinsically expressing deletional EGFR were also hypersensitive to gefitinib (11, 17), and the AKT pathway was more sensitively inhibited by gefitinib as compared with p44/42 MAPK pathway (18). These findings are consistent with the evidence seen in the 293(D) cells. The altered downstream pathway in the cells expressing other types of mutant EGFR was previously reported. The L858R and delL747-P753insS were basically unphosphorylated and these mutants were markedly phosphorylated compared with wild-type EGFR by ligand stimulation (4, 5). Activated AKT signaling pathways, but not MAPK pathway was observed in the transfectants of L858R and delL747-P753insS. Taken together, preferential activation of AKT pathway was commonly observed between these EGFR mutant cells. On the other hand, there were some differences between delE746-A750, L858R, and delL747-P753insS; constitutive active in delE746-A750 vs. hyperresponse to ligand stimulation in L858R and delL747-P753insS. These EGFR mutations except for T790M are considered to be "gain of function," although detailed differential function will be clarified in future studies.

We examined the phosphorylation status of EGFR and its downstream events in PC-9 cells intrinsically expressing deletional mutant EGFR in addition to the ectopic expression system. However, the PC-9 cells also express low levels of wild-type of EGFR. It can thus be considered that these cells mimic the 293(D) cells. In the PC-9 cells, IκB-α is activated. IκB-α binds to NF-κB and suppresses this function (19). Kapoor reported that NF-κB activating signal from EGFR is mediated by the PI3-kinase/AKT pathway (20). We used immunoblotting to investigate the phosphorylation of AKT in the PC-9 cells after EGF stimulation. Increased phosphorylation of AKT was induced even under unstimulated conditions and considered that the activation (or phosphorylation) of IκB-α occurred via the AKT pathway machinery. Therefore, the phosphorylation of IκB-α is due to the activation of the AKT pathway in the PC-9 cells.

In the PC-9 cells, increased phosphorylation of p44/42 MAPK and ATF-2 (21, 22) was detected with the addition of EGF. In addition, phosphorylation of IκB-α was also increased by the ligand stimulation in the PC-9 cells, suggesting that this signaling pathway might be mediated by wild-type of EGFR.

We demonstrated that deletional EGFR was hyperphosphorylated and dimerized in a steady state in the 293(D) cells. This mutant is considered to be constitutively active. The activation mutation in EGFR is consistent with that of the c-KIT mutation in GIST that is a target for gleevec (23). The c-KIT mutations in GIST have also been reported as gain-of-function mutations (24). The role of

mutant EGFR and its function in transformation activity and carcinogenesis requires clarification in future studies.

Downstream of the signaling pathway, p44/42 MAPK and AKT pathways are activated in the 293(D) cells, but the AKT pathway was more strongly suppressed by gefitinib. Therefore, the AKT pathway must interact with cellular hypersensitivity to the EGFR targeted tyrosine kinase inhibitor in cells expressing deletional mutant EGFR.

In this study, we focused on the short, in-frame deletional mutant (E746_A750del). Now more than 30 types of mutation have been reported in clinical lung cancer specimens. In the next step, we will examine the biological function of other types of mutants of EGFR differentially, with the aim of selecting clinically meaningful mutations.

ACKNOWLEDGMENTS

This work was supported by funds for the Third Term Comprehensive 10-Year Strategy for Cancer Control and a Grant-in-Aid for Scientific Research from the Ministry of Education, Culture, Sports, Science and Technology of Japan (12217165).

REFERENCES

1. Yarden, Y., and Sliwkowski, M. X. (2001) Untangling the ErbB signalling network. *Nat. Rev. Mol. Cell Biol.* **2**, 127–137

2. Tanner, K. G., and Kyte, J. (1999) Dimerization of the extracellular domain of the receptor for epidermal growth factor containing the membrane-spanning segment in response to treatment with epidermal growth factor. *J. Biol. Chem.* **274,** 35,985–35,990

3. Paez, J. G., Janne, P. A., Lee, J. C., Tracy, S., Greulich, H., Gabriel, S., Herman, P., Kaye, F. J., Lindeman, N., Boggon, T. J., et al. (2004) EGFR mutations in lung cancer: correlation with clinical response to gefitinib therapy. *Science* **304,** 1497–1500

4. Lynch, T. J., Bell, D. W., Sordella, R., Gurubhagavatula, S., Okimoto, R. A., Brannigan, B. W., Harris, P. L., Haserlat, S. M., Supko, J. G., Haluska, F. G., et al. (2004) Activating mutations in the epidermal growth factor receptor underlying responsiveness of non-small-cell lung cancer to gefitinib. *N. Engl. J. Med.* **350,** 2129–2139

5. Sordella, R., Bell, D. W., Haber, D. A., and Settleman, J. (2004) Gefitinib-sensitizing EGFR mutations in lung cancer activate anti-apoptotic pathways. *Science* **305,** 1163–1167

6. Arao, T., Fukumoto, H., Takeda, M., Tamura, T., Saijo, N., and Nishio, K. (2004) Small in-frame deletion in the epidermal growth factor receptor as a target for ZD6474. *Cancer Res.* **64,** 9101–9104

7. Tracy, S., Mukohara, T., Hansen, M., Meyerson, M., Johnson, B. E., and Janne, P. A. (2004) Gefitinib induces apoptosis in the EGFRL858R non-small-cell lung cancer cell line H3255. *Cancer Res.* **64,** 7241–7244